crystals

MDPI

Article

Effect of External Magnetic Field on the Forming, Microstructure and Property of TC4 Titanium Alloy during the Directed Energy Deposition Arc Additive Manufacturing

Yubo Bao [1,2,*], Hongwei Sun [2], Xiaoyu Cai [1], Sanbao Lin [1] and Chao Chen [3]

[1] State Key Laboratory of Advanced Welding and Joining, Harbin Institute of Technology, Harbin 150001, China
[2] Jiangsu Automation Research Institute, Lianyungang 222006, China
[3] College of Mechanical and Electrical Engineering, Northeast Forestry University, Harbin 150040, China
* Correspondence: author: baoyubo2022@126.com; Tel.: +86-189-1124-0621; Fax: +86-010-8852-9073

Abstract: In this work, the thin wall components of TC4 titanium alloy were produced by using external magnetic field hybrid gas metal welding (EM-GMAW). The effect of the external magnetic field on the forming, microstructure, and property of wire arc additively manufactured TC4 titanium alloy was studied in detail. The results showed that the height of the average deposition layer of EM-GMAW was less than that of GMAW and decreased with the increase of magnetic excitation current, and the width of the average deposition layer of EM-GMAW was greater than that of GMAW. The microstructure of the deposition layer consisted of fine α phase and coarse β grains. Compared with the traditional GMAW, the coarse β grain size in the EM-GMAW was reduced obviously. The maximum size of β grain was decreased by 100μm when the magnetic excitation current of 3A was used. In addition, the EM-GMAW tensile strength in the transverse and horizontal was increased by around 20 MPa and 100 MPa, respectively, compared with that of GMAW.

Keywords: titanium alloy; arc additive manufacturing; magnetic field; microstructure; property

Citation: Bao, Y.; Sun, H.; Cai, X.; Lin, S.; Chen, C. Effect of External Magnetic Field on the Forming, Microstructure and Property of TC4 Titanium Alloy during the Directed Energy Deposition Arc Additive Manufacturing. *Crystals* **2023**, *13*, 235. https://doi.org/10.3390/cryst13020235

Academic Editors: Soumya Sridar, Avinash Hariharan and Shiva Sekar

Received: 3 January 2023
Revised: 16 January 2023
Accepted: 20 January 2023
Published: 29 January 2023

1. Introduction

TC4 (Ti-6Al-4V) titanium alloy belongs to α + β double-phase titanium alloys and has become the flagship alloy in the titanium alloy industry due to its good performance such as heat resistance, strength, plasticity, toughness, formability, weldability, corrosion resistance, and biocompatibility. The use of this alloy has accounted for 75–85% of all titanium alloys [1,2]. Directed energy deposition arc additive manufacturing (DED-AAM) uses layer-by-layer surfacing to manufacture dense metal solid components. Because DED-arc additive manufacturing utilizes arc as the energy beam and has high heat input and fast forming speed, it is suitable for the low-cost, efficient, and rapid near-net forming of large-size complex components, and has great engineering potential in the field of titanium alloy forming and manufacturing.

When the TC4 titanium alloy wire was used for DED-arc additive manufacturing, the titanium alloy additive parts have good formability, but there are obvious shortcomings such as significant anisotropy, coarse microstructure, etc. [3]. In order to improve the microstructure of the deposited parts, some additional processing processes or energy fields were introduced into DED-arc additive manufacturing processes.

For the additional processing processes, the technology of rolling [4,5] and mechanical hammering [6] was employed to improve the surface microstructure of additive manufacturing samples based on the theory of severe plastic deformation. Previous research [7–9] indicated that epitaxial solidification was the main reason for the formation of coarse columnar β grain during titanium alloy additive manufacturing. Severe plastic deformation could refine the surface microstructure [10]. The refinement microstructure could restrain the grain growth in the epitaxial solidification. Martina et al. [4] studied the microstructure

of interpass rolled wire plus arc additive manufacturing Ti-6Al-4V components. They found that the coarse columnar β grain transit to fine equiaxed grains and the grain size was obviously reduced when the interpass rolled wire was added during the DED-AAM. Similar results were also reported by Mcandrew A.R et al. [6]. Hnnige J R et al. [5] used the ForgeFixXP pneumatic mechanical hammering system to treat the surface of Ti-6AL-4V alloy additive manufacturing samples. They indicated that although the mechanical hammering depth was less than the depth of the molten pool, the centimeter columnar grains were also effectively refined to equiaxed grains. However, due to additional rolling and mechanical hammering, the DED-AAM device became complex and had poor flexibility. Therefore, some energy field device in relatively simple structure was introduced into the additive manufacturing process to control the solidification process of the molten pool, as reported by researchers [11–13].

Controlling the solidification process of the molten pool by an additional energy field was earlier used in casting and welding fields [14,15]. Ultrasonic and electromagnetic fields were commonly used to control the solidification process of the molten pool based on the theories of acoustic cavitation and electromagnetic oscillation. Chen et al. [16] studied the influence of ultrasonic on the solidification process of the molten pool during the TIG welding processes. Under the action of ultrasonic, the refinement microstructure was obtained due to acoustic cavitation broken dendrite. Todaro C J et al. [17] reported the grain refinement of stainless steel in ultrasound-assisted additive manufacturing. However, the distance between the ultrasound horn and the molten pool was not constant during the welding or additive manufacturing, so, the effect of ultrasound on the solidification process of the molten pool was uneven. By contrast, the electromagnetic field could perform uniform control of the molten pool due to the synchronous movement of the electromagnetic field and heat source [14]. Electromagnetic oscillation can usually refine the microstructure and improve the welded joint property during welding [18]. Sundaresan et al. [19] reported grain refinement of gas tungsten arc welds in α–β titanium alloys by using magnetic arc oscillation. Electromagnetic oscillation could stir the molten pool and further control the solidification process. Wang et al. [11] indicated that the stirring effect of the magnetic field during Inconel 625 superalloy fabricated by DED-arc additive manufacturing refines dendritic crystal size.

The above research on how to control the microstructure and properties of TC4 titanium alloy arc additive manufacturing components has attracted much attention. Electromagnetic oscillation usually can refine the microstructure during welding or additive manufacturing. Therefore, it may be concluded that using electromagnetic oscillation also could improve the microstructure and properties of TC4 titanium alloy arc additive manufacturing components. This paper proposes to use the method of an external axial electromagnet to control TC4 titanium alloy GMAW additive manufacturing processes. The influence of magnetic field on TC4 titanium alloy GMAW additive manufacturing components was explored from the forming, microstructure, and property of the component.

2. Experiment Material and Method

In this paper, a Ti-6Al-4V titanium alloy welding wire with a diameter of 1.2 mm was used for arc additive manufacturing. Ti-6Al-4V titanium alloy with a dimension of 100 mm × 12 mm × 12 mm was selected as the substrate. Its chemical composition (at%) is Al (5.5~6.8%), V (3.5~4.5%), Fe (0.30% or less), O (0.20% or less), C (0.10% or less), N (0.05%) or less and Ti (allowance) [1]. The external longitudinal magnetic field hybrid gas metal welding additive manufacturing (M-GMAW-AM) system is shown in Figure 1. The system mainly includes a GMAW power source, an external longitudinal magnetic field composite GMAW welding torch, and a walking platform. The coil turns of the longitudinal magnetic field are 140, and the magnetic excitation current ranges from 1A to 3A. Under the action of the external longitudinal magnetic field, droplet transition and molten pool solidification will be affected by an external electromagnetic force.

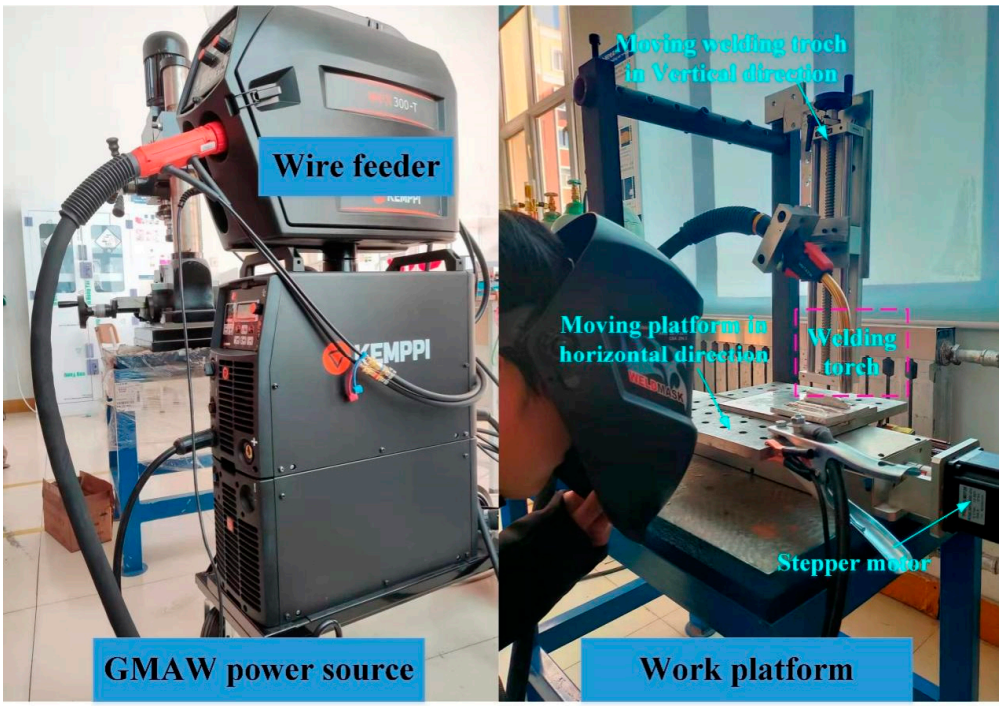

Figure 1. The external longitudinal magnetic field hybrid gas metal welding additive manufacturing (M-GMAW-AM) system.

During the DED-AAM, the moving platform had horizontal movement by controlling the stepper motor obtained from different deposition speeds. In this work, a deposition speed of 5 mm/s and a shielding gas rate of 15 L/min were used. The distance between the end of the welding torch and the deposition layer was kept at 15 mm at all times and obtained by moving the welding torch in the vertical direction, as shown in Figure 1. Table 1 shows the detailed parameters of Ti-6Al-4V alloy in M-GMAW-AW. Voltage is the fixed parameter (30 V). Parameter variables include wire feed speed (7–9 m/min) and excitation current (1–3A).

Table 1. Parameters of Ti-6Al-4V alloy during the magnetic field assisted DED-AAM.

No.	Voltage (V)	Wire Feed Speed (m/min)	Excitation Current (A)
1	30	7	0
2			1
3			2
4			3
5		8	0
6			1
7			2
8			3
9		9	0
10			1
11			2
12			3

The single deposition test was carried out using the process parameters in Table 1. The surface of the deposition layer was photographed and observed by a high-resolution camera. Metallographic specimen preparation and microstructure observation were performed on the cross-section of the deposition components. The specimens for metallographic observation were prepared by the following steps. First, metallographic specimens were cut by the wire-cutting process. Then, the metallographic specimens were ground sequentially with sandpaper of the type of 240 to 1500 grit. The metallographic specimens needed to

go through a polishing process after grinding on sandpaper. Finally, the microstructure could be observed after the metallographic specimens were corroded with a 4% nitric acid alcohol solution.

3. Results and Discussion

3.1. Single Deposition Forming

Figure 2 shows the surface morphology of the titanium alloy single deposition layer under different process parameters. During the deposition process, the I_M value was adjusted in real time at the green line. For example, at the left of Figure 2a is expressed the image of I_M = 0 A. At the right of Figure 2a is expressed the image of I_M = 1 A. When the wire feeding speed is 7 m/min, the surface morphology of the titanium alloy deposition layer under different magnetic excitation currents is shown in Figure 2a,b. The deposition layer forming quality of GMAW and M-GMAW with a magnetic excitation current of 1 A is better. When the magnetic excitation current increases to 2 A and 3 A, the width of the deposition layer increases obviously. Figure 2c,f show the surface morphology of the deposition layer with the wire feeding speed of 8 m/min and 9 m/min, respectively. It can be found that the width of the deposition layer increases significantly with the increase of the wire feeding speed. When the wire feeding speed is constant, the width of the deposition layer increases with the increase of the magnetic excitation current.

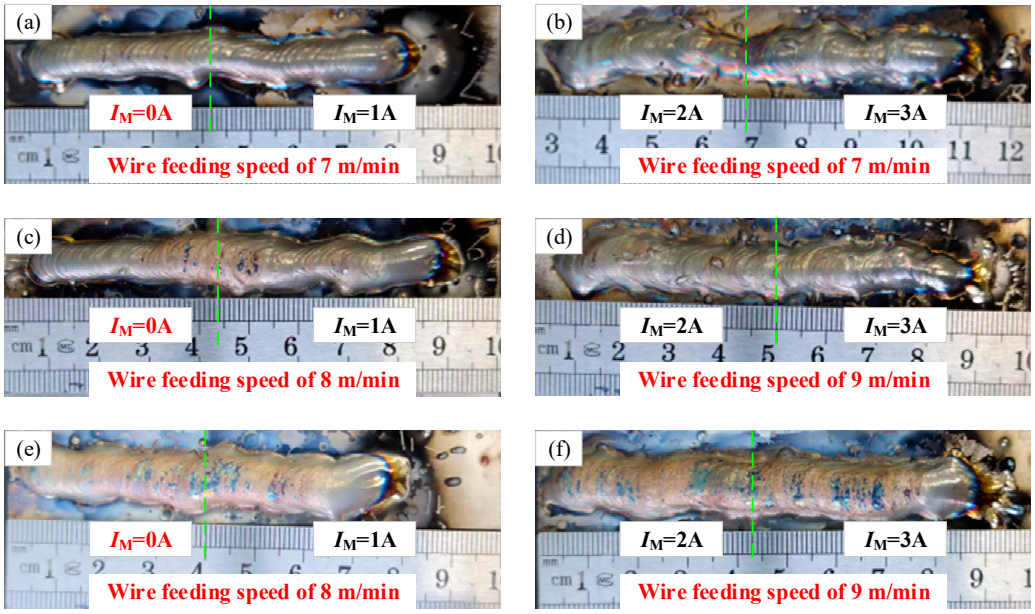

Figure 2. Surface morphology of the titanium alloy single deposition layer: (**a**,**b**) shows the wire feeding speed of 7 m/min, (**c**,**d**) shows the wire feeding speed of 8 m/min, (**e**,**f**) shows the wire feeding speed of 9 m/min.

Figure 3 shows the cross-sectional morphologies of the titanium alloy deposition layer under different process parameters. Figure 3a shows the cross-section morphologies of the titanium alloy deposition layer under different magnetic excitation currents at a wire feeding speed of 7 m/min. The cross-sectional width of the M-GMAW deposition layer increases more than that of the GMAW deposition layer. With the increase of magnetic excitation current, the deposition layer width increases significantly, and the grain size of the M-GMAW deposition layer is significantly smaller than that of the GMAW. The cross-sectional morphologies variation of the titanium alloy deposition layer with the wire feeding speed of 8 m/min and 9 m/min are consistent with that of the wire feeding speed of 7 m/min.

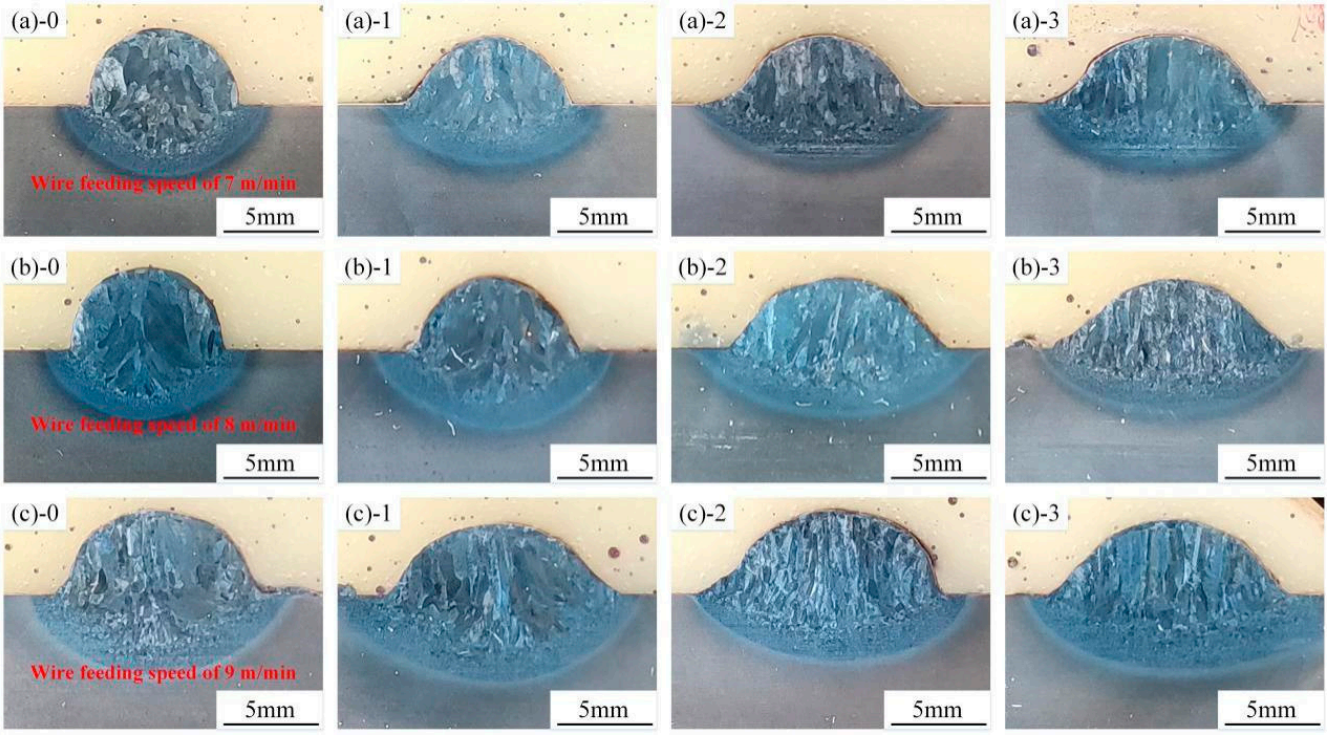

Figure 3. Cross-sectional morphologies of titanium alloy deposition layer: (**a**) Wire feeding speed of 7 m/min with different magnetic excitation currents, (**b**) Wire feeding speed of 8 m/min with different magnetic excitation currents, (**c**) Wire feeding speed of 9 m/min with different magnetic excitation currents.

Figure 4 shows the geometric parameters of the titanium alloy cross-sectional deposition layer under different process parameters. A schematic diagram of cross-sectional geometric parameter measurement is shown in Figure 4d. When the wire feeding speed is 7 m/min, the cross-sectional geometric parameters of the titanium alloy deposition layer under different magnetic excitation currents are shown in Figure 4a,b. The width and height of the GMAW deposition layer are 8 mm and 4.9 mm, respectively. When M-GMAW is used, the cross-section width of the deposition layer increases significantly with the increase of magnetic excitation current. When the magnetic excitation current increases to 3 A, the deposition layer width reaches 10.7 mm. The deposition layer height of M-GMAW has no obvious change with the increase of magnetic excitation current. However, it decreases compared with the GMAW. When the wire feeding speed is 8 m/min, the width and height of the GMAW deposition layer are 8.6 mm and 4.9 mm, respectively. After adding a magnetic field, the variation law of cross-sectional geometric parameters of the M-GMAW deposition layer with the wire feeding speed of 8 m/min is consistent with that of the M-GMAW deposition layer with the wire feeding speed of 7 m/min. When the wire feeding speed is 9 m/min, the width and height of the GMAW deposition layer are 10.9 mm and 5.2 mm, respectively, which are increased compared to the GMAW deposition layer with the wire feeding speed of 7 and 8 m/min. Similarly, the variation of the cross-sectional geometric parameters of the deposited layer with a magnetic field added at a feeding speed of 9 m/min is consistent with that at a feeding speed of 7 m/min.

The above results showed that the geometric forming of the deposition layer has changed significantly after different GMAW parameters are introduced into the magnetic field, and has the same change trend, that is, the width of the deposition layer increases and the height decreases under the action of a magnetic field. The literature [20] indicates that the arc shape would rotate under the action of an external magnetic field. The rotated arc shape could enhance the spreading of the melting pool, so the width of the deposited layer would increase.

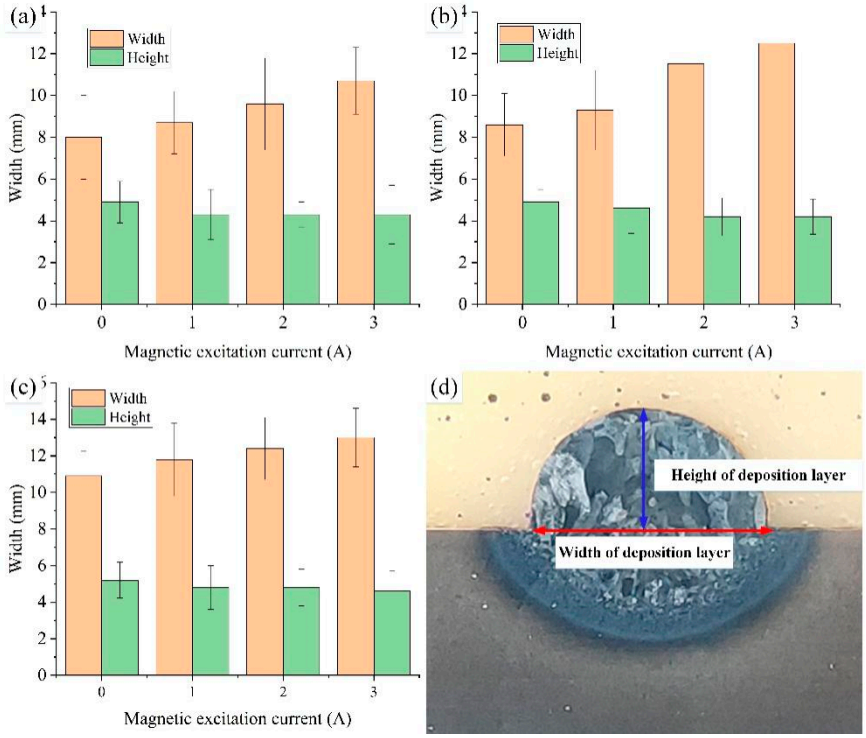

Figure 4. Geometric parameters of cross-sectional of titanium alloy deposited layer under different process parameters: (**a**) Wire feeding speed of 7 m/min, (**b**) Wire feeding speed of 8 m/min, (**c**) Wire feeding speed of 9 m/min, (**d**) Schematic diagram of geometric dimension measurement.

3.2. Thin-Walled Additive Manufacturing Component

By researching and observing the surface forming and the cross-sectional morphology of a single deposition layer, the basic forming law was mastered. In the following, this paper will select the wire feeding speed of 7 m/min as an example to carry out the thin-walled deposition test by using GMAW and M-GMAW under the different magnetic excitation currents. The thin-walled additive manufacturing components are shown in Figure 5.

As shown in Figure 5a, GMAW components with a total deposition layer height of 4.9 cm can be achieved by depositing 15 layers. The average deposition layer height is about 0.327 cm. As shown in Figure 5b, when the magnetic field with a magnetic excitation current of 1 A is introduced, the component height of 4.41 cm needs a deposit of 14 layers. The average layer height is about 0.315 m. As shown in Figure 5c, when the magnetic field with a magnetic excitation current of 2 A is introduced, the component height of 4.18 cm needs a deposit of 14 layers. The average layer height is about 0.298 cm. As shown in Figure 5d, when the magnetic field with a magnetic excitation current of 3 A is introduced, the component height of 4.59 cm needs a deposit of 16 layers. The average layer height is about 0.287 cm.

3.3. Microstructure

This part will observe and analyze the microstructure, such as the phase distribution, grain orientation, grain size, etc., of the middle section of the component under different process parameters.

Figure 6 shows the phase distribution of titanium alloy thin-walled additive manufacturing components under different process parameters. The red area represents the α phase and the green area represents the β phase in the figure. In the GMAW additive manufacturing component, the ratio of α phase and β phase is 99.2% and 0.08%, respectively (Figure 6a). As shown in Figure 6b, when the magnetic excitation current is 1 A, the ratio of α phase and β phase is 99.7% and 0.03%, respectively. As shown in Figure 6c, when the magnetic excitation current is 2 A, the ratio of α phase and β phase is 99.8% and 0.02%,

respectively. As shown in Figure 6d, when the magnetic excitation current is 3 A, the ratio of α phase and β phase is 99.2% and 0.08%, respectively. It can be found that the ratio of the α phase is greater than that of the β phase. In the additive manufacturing process, the heating temperature reaches the transition temperature of the α phase, and the solidification of the molten pool is a rapid cooling process. During the rapid cooling process, it is too late to transform the amount of α phase into β phase. Hence, the main phase of the component is α phase, and only a small amount of β phase exists. In addition, after introducing an external magnetic field, the ratio between α phase and β phase is significantly unchanged, indicating that the magnetic field has little effect on the phase ratio.

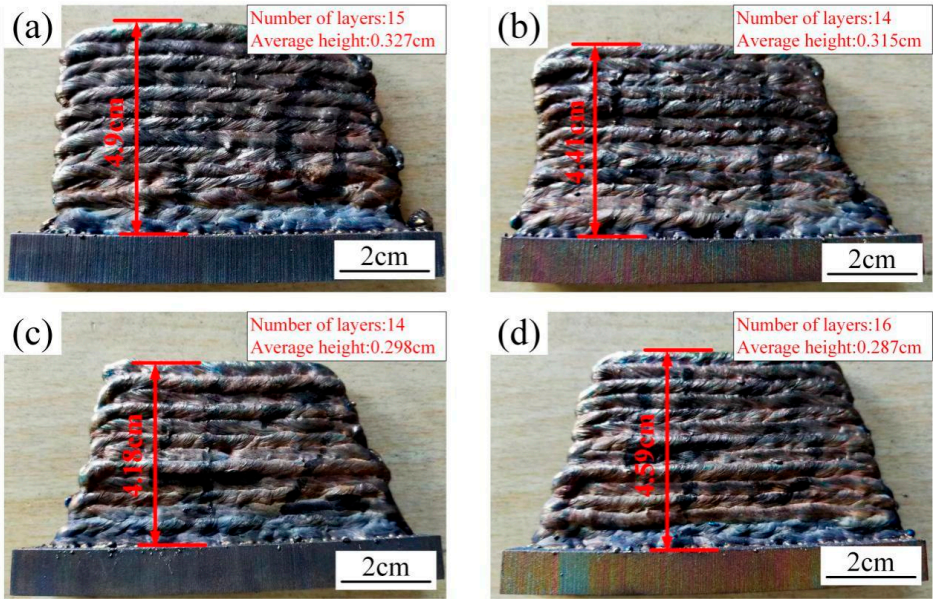

Figure 5. Macro forming of titanium alloy DED-AAM component with the wire feeding speed of 7 m/min: (**a**) I_M = 0 A, (**b**) I_M = 1 A, (**c**) I_M = 2 A, (**d**) I_M = 3 A.

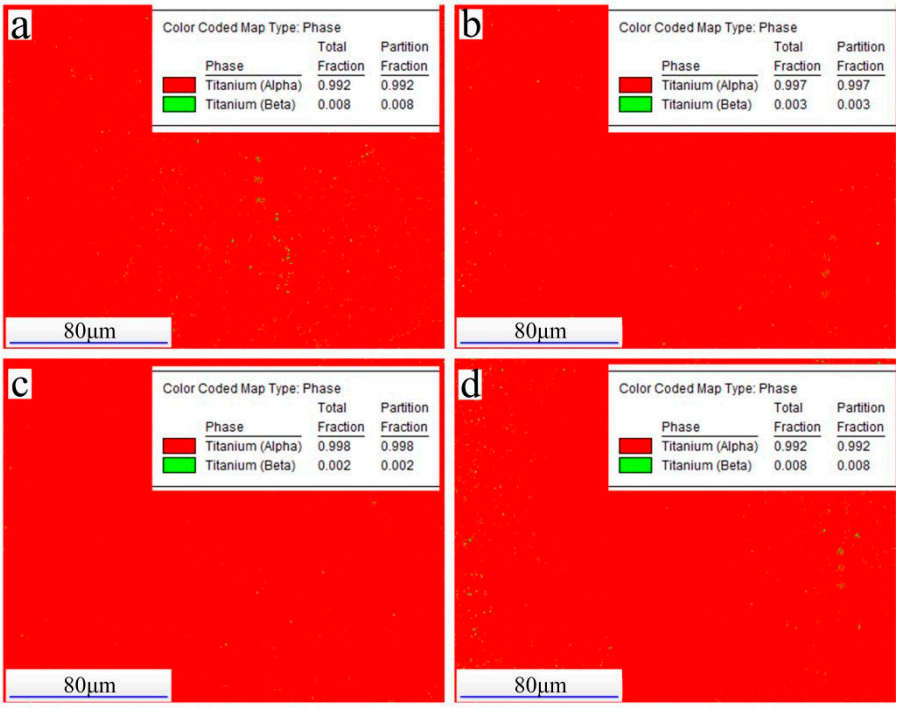

Figure 6. Phase distribution of titanium alloy DED-AAM component with the wire feeding speed of 7 m/min: (**a**) I_M = 0 A, (**b**) I_M = 1 A, (**c**) I_M = 2 A, (**d**) I_M = 3 A.

Grain morphology and crystal orientation of titanium alloy thin-walled additive manufacturing components under different process parameters can be observed in Figure 7. As shown in Figure 7a, the microstructure of GMAW mainly consists of coarse β columnar crystals with fine α phase distributed in the grains. Figure 7b–d show the grain morphology and crystal orientation of M-GMAW at magnetic excitation current 1 A, 2 A, and 3 A, respectively. It can be observed that compared with GMAW, the maximum grain size of M-GMAW is significantly reduced, and the crystal orientation distribution becomes more disorderly.

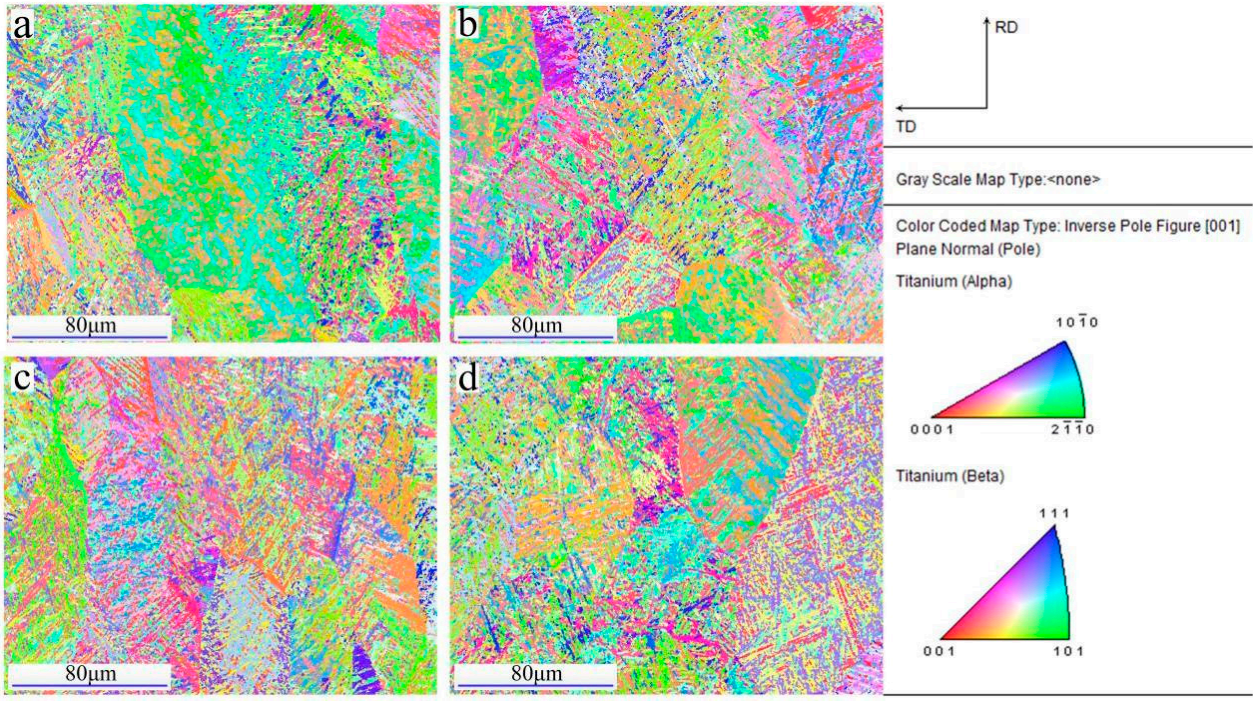

Figure 7. Grain morphology and crystal orientation of titanium alloy DED-AAM component with the wire feeding speed of 7 m/min: (**a**) I_M = 0 A, (**b**) I_M = 1 A, (**c**) I_M = 2 A, (**d**) I_M = 3 A.

The size of α and β phase in the titanium alloy DED-AAM component with the wire feeding speed of 7 m/min can be seen in Figure 8. It can be seen that two distribution ranges in phase size are, respectively, ~100 μm and 100 μm~. From Figure 7, β phase size was greater than that of α phase. Therefore, the phase size distribution ranges of ~100 μm expressed the size change of α phase, and the phase size distribution ranges of 100 μm~ expressed the size change of β phase.

As shown in Figure 8a, the maximum size of the β phase in the GMAW is about 280 μm and the average size in α and β phase is 38.8676 μm. When the magnetic field of magnetic excitation current of 1 A is introduced, the maximum β phase size and average size in α and β phase is about 200 μm and 32.2712 μm, respectively (Figure 8b). When the magnetic field of the magnetic excitation current of 2 A is introduced, the maximum β phase size and average size in the α and β phase are about 240 μm and 33.8005 μm, respectively (Figure 8c). When the magnetic field of the magnetic excitation current of 3 A is introduced, the maximum size of the β phase and average size in α and β phase are about 180 μm and 38.3477 μm, respectively (Figure 8c). Compared with GMAW, the maximum size of the β phase and the average size of the phase decrease after the introduction of the magnetic field. When the magnetic excitation current is 3 A, the maximum size of the β phase decreases the most, by 100 μm; when the magnetic excitation current is 1 A, the average size of the phase decreases the most, by 6.5964 μm.

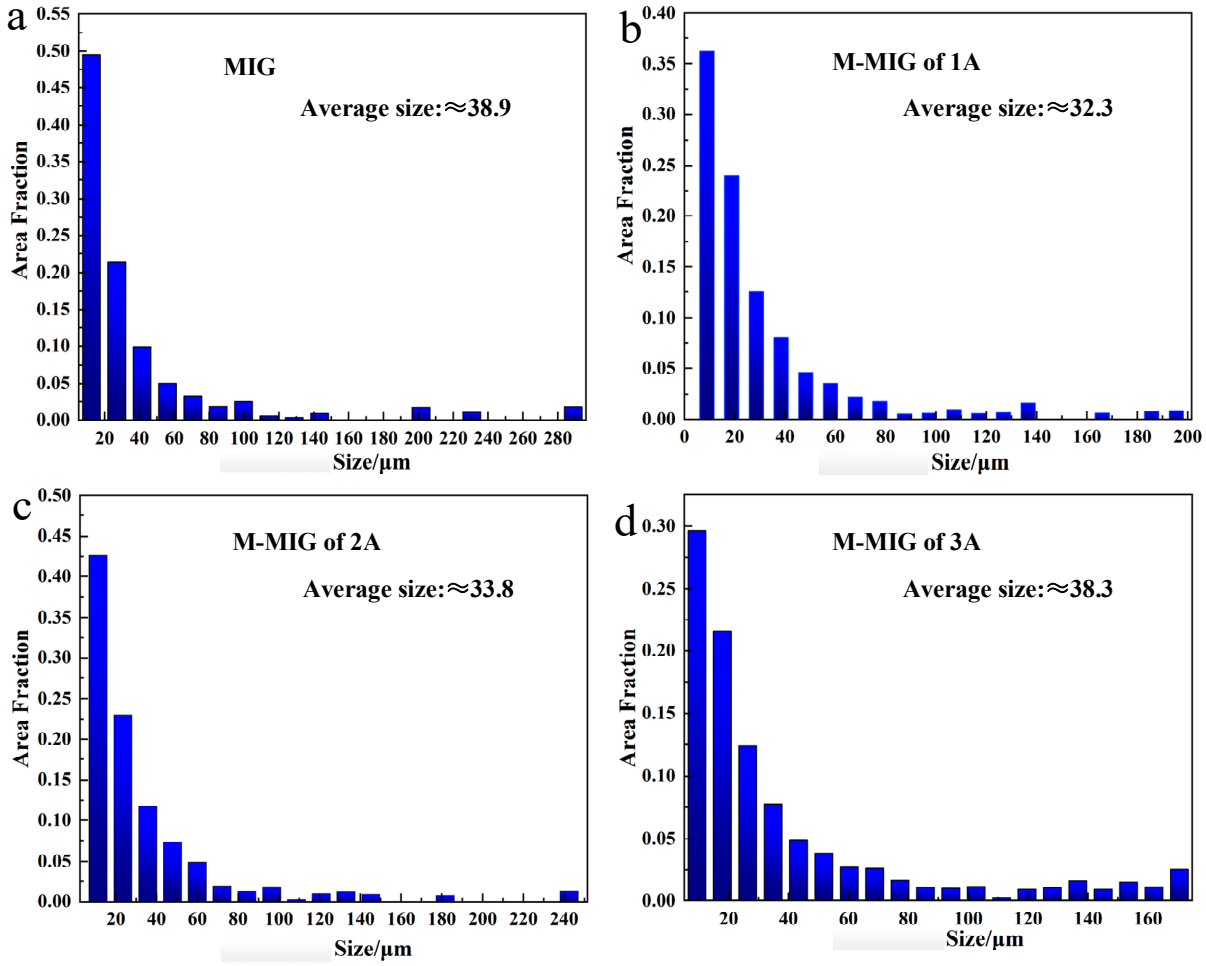

Figure 8. The size of α and β phase in the titanium alloy DED-AAM component with the wire feeding speed of 7 m/min: (**a**) I_M = 0 A, (**b**) I_M = 1 A, (**c**) I_M = 2 A, (**d**) I_M = 3 A.

From the above results of microstructure, the grain size could be refined by adding an external magnetic field. Hunt et al. [21] indicated that the coarse columnar crystal transferred into the fine equiaxed crystal could be explained by Formula (1).

$$G_L \leq 0.061 N_0^{1/3} \left[1 - \frac{(\Delta T_N)^3}{(\Delta T_c)^3} \right] \Delta T_c \quad (1)$$

where the G_L is the solid-liquid interface temperature gradient, N_0 is the heterogeneous nucleation rate, $\triangle T_N$ is the critical undercooling of homogeneous nucleation, $\triangle T_c$ is the undercooling of the columnar crystal front. Therefore, when the reduction of G_L and $\triangle T_N$, and the increase of N_0 and $\triangle T_c$ were obtained, this was conducive to the transformation from coarse columnar crystal to equiaxed crystal. Under the action of the external magnetic field, the forced convection would be formed in the weld pool, which made the reduction of G_L due to the change of fluid of the weld pool [22]. In addition, the dendrite in the solid-liquid interface was fractured under the electromagnetic stirring, as shown in Figure 9. Broken dendrite would become the nucleating particle to enhance the nucleation rate. Therefore, the refinement grain was obtained by using M-GMAW.

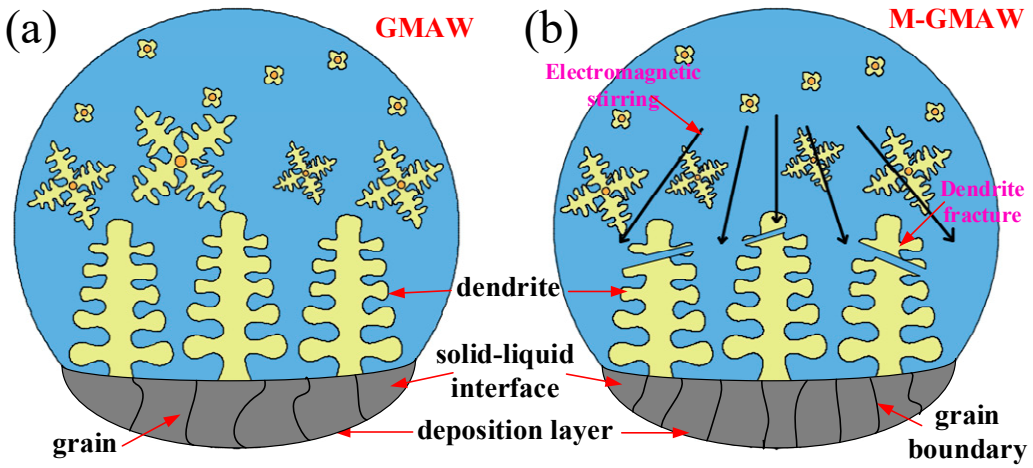

Figure 9. (**a**,**b**) Grain refinement under the action of electromagnetic stirring.

3.4. Mechanical Property

The tensile strength of the titanium alloy thin-walled additive manufacturing component can be seen in Figure 10. It can be seen that the longitudinal tensile strength is greater than the vertical tensile strength. When the magnetic excitation current is 1 A and 2 A, the transverse tensile strength of M-GMAW is obviously greater than that of GMAW, which is increased by about 40 MPa. The longitudinal tensile strength obtained by M-GMAW with the magnetic excitation current of 3 A is increased by around 20 MPa compared with that of GMAW, and its vertical tensile strength is increased by around 100 MPa. The difference between the longitudinal and vertical tensile strength obtained by M-GMAW with the magnetic excitation current of 3 A is the smallest. Previous research [6,7] indicated that anisotropy of titanium alloy components in the WAAM was mainly caused by the coarse β grain. Owing to the coarse β grain growth along the vertical direction, the vertical tensile strength was greater than the longitudinal tensile strength. Therefore, we find that similar results were also obtained in this work.

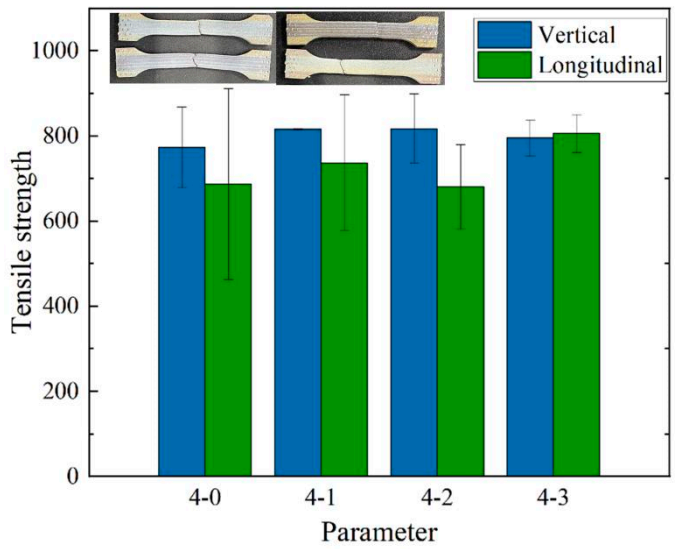

Figure 10. Tensile strength of titanium alloy thin-walled additive manufacturing component.

4. Conclusions

The average deposition layer height of GMAW was about 0.327 cm. The average height of the deposited layer decreased under the magnetic field. When the magnetic excitation current was 3 A, the average layer height of M-GMAW was about 0.287 cm.

The microstructure of the deposition layer consisted of a number of α phases and a little β phase. Compared with GMAW, the maximum phase size and average phase size decreased after the introduction of a magnetic field.

The vertical tensile strength obtained by M-GMAW with the magnetic excitation current of 3 A was increased by around 20 MPa compared with that of GMAW, and its longitudinal tensile strength was increased by around 100 MPa. The difference between the vertical and longitudinal tensile strength obtained by M-GMAW with the magnetic excitation current of 3 A was the smallest.

Author Contributions: Investigation, Y.B.; resources, Y.B.; data curation, H.S.; writing—original draft preparation, Y.B.; writing—review and editing, Y.B.; visualization, C.C.; supervision, X.C., S.L. All authors have read and agreed to the published version of the manuscript.

Funding: This research received no external funding.

Data Availability Statement: Not applicable.

Conflicts of Interest: The authors declare no conflict of interest.

References

1. Chen, C.; Chen, F.; Yang, Y.; Zhang, H. Study on appearance and mechanical behavior of additively manufacturing of Ti–6Al–4V alloy by using cold metal transfer. *CIRP J. Manuf. Sci. Technol.* **2021**, *35*, 250–258. [CrossRef]
2. Chen, C.; Fan, C.; Cai, X.; Lin, S.; Liu, Z.; Fan, Q.; Yang, C. Investigation of formation and microstructure of Ti-6Al-4V weld bead during pulse ultrasound assisted TIG welding. *J. Manuf. Process.* **2019**, *46*, 241–247. [CrossRef]
3. Xia, C.; Pan, Z.; Polden, J.; Li, H.; Xu, Y.; Chen, S.; Zhang, Y. A review on wire arc additive manufacturing: Monitoring, control and a framework of automated system. *J. Manuf. Syst.* **2020**, *57*, 31–45. [CrossRef]
4. Martina, F.; Colegrove, P.A.; Williams, S.W.; Meyer, J. Microstructure of Interpass Rolled Wire + Arc Additive Manufacturing Ti-6Al-4V Components. *Metall. Mater. Trans. A* **2015**, *46*, 6103–6118. [CrossRef]
5. Hönnige, J.R.; Davis, A.E.; Ho, A.; Kennedy, J.R.; Neto, L.; Prangnell, P.; Williams, S. The Effectiveness of Grain Refinement by Machine Hammer Peening in High Deposition Rate Wire-Arc AM Ti-6Al-4V. *Metall. Mater. Trans. A* **2020**, *51*, 3692–3703. [CrossRef]
6. McAndrew, A.R.; Rosales, M.A.; Colegrove, P.A.; Hönnige, J.R.; Ho, A.; Fayolle, R.; Eyitayo, K.; Stan, I.; Sukrongpang, P.; Crochemore, A.; et al. Interpass rolling of Ti-6Al-4V wire+arc additively manufactured features for microstructural refinement. *Addit. Manuf.* **2018**, *21*, 340–349. [CrossRef]
7. Zhu, Y.; Tian, X.; Li, J.; Wang, H. The anisotropy of laser melting deposition additive manufacturing Ti–6.5Al–3.5Mo–1.5Zr–0.3Si titanium alloy. *Mater. Des.* **2015**, *67*, 538–542. [CrossRef]
8. Zhang, Q.; Chen, J.; Lin, X.; Tan, H.; Huang, W.D. Grain morphology control and texture characterization of laser solid formed Ti6Al2Sn2Zr3Mo1.5Cr2Nb titanium alloy. *J. Mater. Process. Technol.* **2016**, *238*, 202–211. [CrossRef]
9. Davis, A.E.; Breheny, C.I.; Fellowes, J.; Nwankpa, U.; Martina, F.; Ding, J.; Machry, T.; Prangnell, P.B. Mechanical performance and microstructural characterisation of titanium alloy-alloy composites built by wire-arc additive manufacture. *Mater. Sci. Eng. A* **2019**, *765*, 138289. [CrossRef]
10. Mashreghi, A.; Ghalandari, L.; Reihanian, M.; Moshksar, M.M. Processing, Strength and Ductility of Bulk Nanostructured Metals Produced by Sever Plastic Deformation: An Overview. *Mater. Sci. Forum* **2009**, *633–634*, 131–150. [CrossRef]
11. Wang, Y.; Chen, X.; Shen, Q.; Su, C.; Zhang, Y.; Jayalakshmi, S.; Singh, R.A. Effect of magnetic Field on the microstructure and mechanical properties of inconel 625 superalloy fabricated by wire arc additive manufacturing. *J. Manuf. Process.* **2021**, *64*, 10–19. [CrossRef]
12. Wang, T.; Mazánová, V.; Liu, X. Ultrasonic effects on gas tungsten arc based wire additive manufacturing of aluminum matrix nanocomposite. *Mater. Des.* **2022**, *214*, 110393. [CrossRef]
13. Zhou, X.; Tian, Q.; Du, Y.; Zhang, Y.; Bai, X.; Zhang, Y.; Zhang, H.; Zhang, C.; Yuan, Y. Investigation of the effect of torch tilt and external magnetic field on arc during overlapping deposition of wire arc additive manufacturing. *Rapid Prototyp. J.* **2021**, *27*, 24–36. [CrossRef]
14. Wu, H.; Chang, Y.; Lu, L.; Bai, J. Review on magnetically controlled arc welding process. *Int. J. Adv. Manuf. Technol.* **2017**, *91*, 4263–4273. [CrossRef]
15. Li, H.; Li, C.; Li, Z.X. Progress in Power Ultrasound Effect on Molten Metal Shaping and Its Visualization. *J. Mater. Eng.* **2017**, *45*, 118–126.
16. Chen, Q.; Lin, S.; Yang, C.; Fan, C.; Ge, H. Grain fragmentation in ultrasonic-assisted TIG weld of pure aluminum. *Ultrason. Sonochemistry* **2017**, *39*, 403–413. [CrossRef] [PubMed]
17. Todaro, C.J.; Easton, M.A.; Qiu, D.; Brandt, M.; StJohn, D.H.; Qian, M. Grain refinement of stainless steel in ultrasound-assisted additive manufacturing. *Addit. Manuf.* **2021**, *37*, 101632. [CrossRef]

18. Sharma, P.; Chattopadhyaya, S.; Singh, N.K. A review on magnetically supported gas metal arc welding process for magnesium alloys. *Mater. Res. Express* **2019**, *6*, 082002. [CrossRef]
19. Sundaresan, S.; Ram, G.D.J. Use of magnetic arc oscillation for grain refinement of gas tungsten arc welds in α–β titanium alloys. *Sci. Technol. Weld. Join.* **1999**, *4*, 151–160. [CrossRef]
20. Chen, C.; Li, W.; Du, W.; Liu, J.; Zhang, H. Feasibility analysis of standing wave ultrasonic-Axial magnetic field hybrid for controlling GTAW arc characteristics. *J. Manuf. Process.* **2022**, *80*, 187–195. [CrossRef]
21. Hunt, J.D. Steady state columnar equiaxed growth of dendrites and eutectic. *Mater. Sci. Eng.* **1984**, *65*, 75–83. [CrossRef]
22. Matsuda, F.; Nakagam, A.H.; Nakata, K. Effect of electromagnetic stirring on weld solidification structure of aluminum alloy. *Trans. Jpn. Weld. Soc.* **1998**, *7*, 111–126.